Fracture Mechanics of Concrete Structures
Proceedingd FRAMCOS-3
AEDIFICATION Publishers, D-79104 Freiburg, Germany

MATERIAL NONLINEAR ANALYSIS OF PRESTRESSED CONCRETE BEAMS WITH CURVED TENDONS

M. Matsukura, M. Ueda, T. Uchiyama and T. Wada
Faculty of Engineering, Hokkaigakuen University, Sapporo, Japan

Abstract
A numerical procedure based on the finite element method for the material nonlinear analysis of prestressed concrete beams with curved tendons is developed. This procedure includes all the stress phenomena of prestressed concrete beams with curved tendons such as tension-softening effect of concrete based on the concept of fracture energy, comprehensive compressive stress-strain curve of confined concrete, yielding of reinforcements and whole bonding stress-slip relationship between reinforcements and concrete. Numerical examples are presented to demonstrate the validity and applicability of the present procedure. The results are compared with experimental results and the analytical results obtained by other investigators.
Key words: Nonlinear analysis, P/C beam, bond-slip, fracture energy

1 Introduction

Previous studies on material nonlinear analysis of prestressed concrete beams with curved tendons, based on the beam theory, include those by Kang et al.(1980), Tanabe et al.(1980) and Nishiyama et al.(1988) However, different assumptions have been made in the analytical methods used in

these reports. For example, in the methods used by Kang et al.(1980) and Nishiyama et al.(1988), it is assumed that the tendon arrangement changes linearly in each element. Regarding the bond action between the tendons and concrete after jacking of the tendons, Kang et al. assume there is a perfect bond, while Nishiyama et al. assume there is an unbonded state. On the other hand, the method used by Tanabe et al.(1980), which treats curvilinearity of tendons, has the disadvantage that bond properties between tendons and concrete can only be set at one value throughout the length of the member.

The aim of the present study is to clarify the displacements, stresses and strains acting on the concrete and reinforcements, and the bond stresses and slips between the concrete and reinforcements in prestressed concrete beams through all ranges of elastic, inelastic, peak load and post-peak load. One of the authors previously proposed a method, based on the finite element method, for analyzing the elastic bending problem of prestressed concrete beams with curved tendons that took into account the bond-slip of tendons. In the present study, this method was expanded to material nonlinear analysis using the incremental displacement method. The method presented here can be used to analyze all stress phenomena occurring in prestressed concrete beams with curved tendons; i.e., 1) the tension-softening effect of concrete based on the concept of fracture energy, 2) the behavior of the comprehensive stress-strain curve of confined concrete on the compression side, 3) yielding of reinforcements (steel reinforcing bars and tendons), and 4) the complete relationship of bonding stress-slip between reinforcements and concrete.

Some numerical examples are presented to examine the validity and applicability of the proposed analytical method, and these results are compared with past experimental results and with the analytical results of other investigators.

2 Fundamental assumptions for analysis

The following fundamental assumptions were made for the present analysis:

(1) The proposed analytical method is based on the small displacement theory according to Kirchhoff hypothesis, and therefore it is assumed that the concrete cross section remains as a plane after loading.

(2) The bending and axial force are assumed

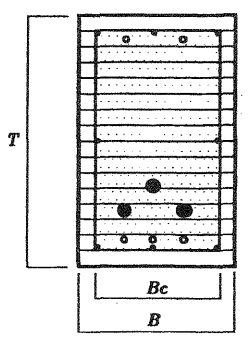

Fig. 1. Idealized Cross-Section

to dominate the deformation of the members. Here, transverse shear deformation is not taken into account.

(3) The layered element method is used,
and the concrete cross section is subdivided into multilayers with confined areas (Fig. 1) closed in by stirrup steel.

(4) Reinforcements (steel bars and tendons) have a curved shape and are arranged in m-layers (variable) in the concrete cross section along the span direction.

(5) Bond-slip occurs along the curve of the reinforcements, between the concrete (which contains grouted cement paste) and each reinforcement layer.

3 Material properties

3.1 Stress-strain relationship of concrete

Compression side — A mathematical model of the stress-strain curve of concrete on the compression side is shown in Fig. 2(a). The ascending part of the monotonic loading curve is expressed by the following equation proposed by Saenz(1974):

$$\sigma_c = \frac{E_{co}\,\epsilon_c}{1+(\frac{E_{co}}{E_{cs}}-2)\frac{\epsilon_c}{\epsilon_{cc}}+(\frac{\epsilon_c}{\epsilon_{cc}})^2} \tag{1}$$

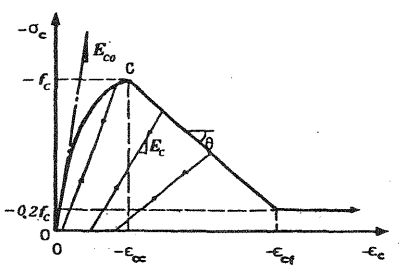

(a) Comprresion Stress-Strain Curve of Concrete

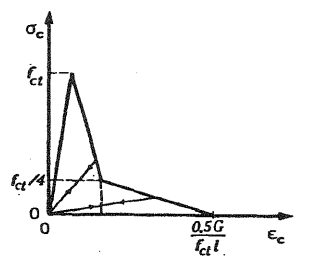

(b) Tension-Softening Curve of Concrete

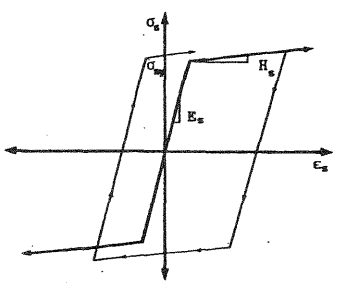

(c) Stress-Strain Curve of Reinforcements

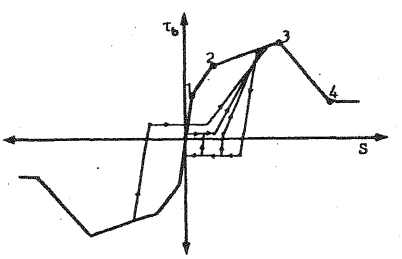

(d) Bond-Slip Curve

Fig. 2. Modeling of Material Properties

where E_{co} = the initial modulus; E_{cs} = the secant modulus at point C in the figure; f_c = the compressive strength of concrete; ϵ_{cc} = the strain at point C.

The inclination angle θ of the descending part in the figure is determined by *the Modified Kent and Park Model.* Also, it is assumed that the value E_c of the unloading path from the monotonic loading curve is reduced by the fracture parameter K_o proposed by Okamura et al.(1991), depending on the magnitude of strain ϵ_{cp} at the start of unloading: $E_c = K_0 E_{co}$.

Tension side — It is known that tensile strength decreases according to the strain ϵ_{cp} at the unloading-start point from the compressive monotonic loading curve. Based on the proposition by Okamura et al.(1991), we define the tensile strength f_{ct} of concrete as

$$f_{ct} = \left(-0.8967\frac{\epsilon_{cp}}{\epsilon_{cc}}\right) f_t \tag{2}$$

where f_t = experimental uniaxial-tensile strength of concrete.

Fig. 2(b) shows a mathematical model of the stress-strain curve of concrete on the tension side, including the tension-softening part, after cracking. The tension-softening curve was proposed by Uchida et al., based on fracture energy, and is known as *the A 1/4 Model.* The unloading- and reloading-paths from the softening curve are also shown.

3.2 Stress-strain relationship of reinforcements

Fig. 2(c) shows the bilinear stress-strain relationship for the reinforcements (steel reinforcing bars and tendons) used in this study. The assumed unloading path is also shown.

3.3 Bond stress-slip relationship

Fig. 2(d) shows a mathematical model of the bond stress-slip relationship between the reinforcement (steel reinforcing bars and tendons) layer and concrete, including the cyclic paths of unloading and reloading. This mathematical model has already been applied by one of the authors to the problem of bond-slip between steel reinforcing bars and concrete, and the fitness of the model has been confirmed. In this study, the coordinate values of points $1 \sim 4$ in the figure for determining the monotonic loading curve were determined by the CEB-FIP model code 1990(1993).

4 General description of analytical method

4.1 Incremental functional

The incremental total potential energy functional for prestressed concrete beams with curved tendons, in the case where the concrete cross section is expressed as a layered element and bond-slip of reinforcements is taken into account, is given by the following equation.

$$\Delta\Pi = \frac{1}{2}\int_0^l \Bigg[\Bigg\{ \sum_{i=1}^{N_c} B_c \Delta t_i E_{ccti} + \sum_{i=1}^{N_k} B_{ki} \Delta t_i E_{ckti} + \sum_{i=1}^{m} A_{si} E_{si} \sqrt{1+\left(\frac{dh_{si}}{dx}\right)^2} \Bigg\} \left(\frac{d\Delta u}{dx}\right)^2$$
$$-2\Bigg\{ \sum_{i=1}^{N_c} B_c \Delta t_i E_{ccti} z_i + \sum_{i=1}^{N_k} B_{ki} \Delta t_i E_{ckti} z_i$$
$$+ \sum_{i=1}^{m} A_{si} E_{si} h_{si} \sqrt{1+\left(\frac{dh_{si}}{dx}\right)^2} \Bigg\} \frac{d\Delta u}{dx}\frac{d^2\Delta w}{dx^2} + 2\sum_{i=1}^{m} \Bigg\{ A_{si} E_{si} \left(\frac{d\Delta u}{dx}\frac{d\Delta S_i}{dx}$$
$$- h_{si}\frac{d^2\Delta w}{dx^2}\frac{d\Delta S_i}{dx} \right) \Bigg\} + \Bigg\{ \sum_{i=1}^{N_c} B_c \Delta t_i E_{ccti} z_i^2 + \sum_{i=1}^{N_k} B_{ki} \Delta t_i E_{ckti} z_i^2$$
$$+ \sum_{i=1}^{m} A_{si} E_{si} h_{si}^2 \sqrt{1+\left(\frac{dh_{si}}{dx}\right)^2} \Bigg\} \left(\frac{d^2\Delta w}{dx^2}\right)^2$$
$$+ \sum_{i=1}^{m} \Bigg\{ \left(A_{si} E_{si} / \sqrt{1+\left(\frac{dh_{si}}{dx}\right)^2} \right) \left(\frac{d\Delta S_i}{dx}\right)^2 + A_{bsi} K_{bi} \sqrt{1+\left(\frac{dh_{si}}{dx}\right)^2} (\Delta S_i)^2 \Bigg\} \Bigg] dx$$
$$- \int_0^l \Bigg\{ \Delta P_u \frac{d\Delta u}{dx} + \Delta q_z \Delta w + \sum_{i=1}^{m} \left(\Delta P_{Si} \frac{d\Delta S_i}{dx} \right) \Bigg\} dx \qquad (3)$$

where l = element length; B_c = width of a concrete cross section in the confined area; E_{ccti} = tangent modulus of the i-th layer of concrete in the confined area; N_c = total number of concrete layers in the confined area; B_{ki} = width of the i-th concrete layer outside the stirrup steel; E_{ckti} = tangent modulus of the i-th concrete layer outside the stirrup steel; N_k = total number of concrete layers outside the confined area; Δt_i = thickness of the i-th concrete layer; A_{si} = cross-sectional area of the i-th reinforcement (steel reinforcing bars and tendons) layer; E_{si} = tangent modulus of the i-th reinforcement layer; K_{bi} = tangent bond modulus of the i-th reinforcement layer; A_{bsi} = bond area per unit length of the i-th reinforcement layer; m = total number of reinforcement layers; Δu = incremental displacement of the beam in the direction of the axis of member; Δw = incremental displacement of the beam in the vertical direction; ΔS_i = incremental slip displacement along the curve of the i-th reinforcement layer; ΔP_u = incremental distributed load in the direction of the axis of member; ΔP_{si} = incremental jacking force of the i-th reinforcement layer; and Δq_z = incremental distributed load in the vertical direction.

4.2 Assumed curve of reinforcement

The curve of reinforcement (steel reinforcing bars and tendons) is depicted as a quadratic curve, and as long as the curve is continuous, it is assumed that the curve may differ for each finite element.

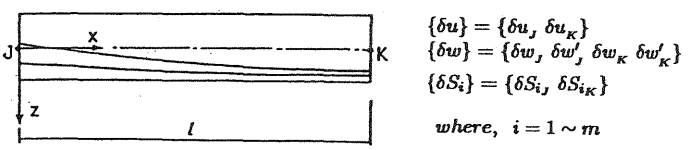

Fig. 3. Prestressed Concrete Beam Element

$$h_{si} = a_i + b_i x + c_i x^2 \tag{4}$$

where h_{si} = vertical distance from the reference axis of the beam in the $i-$th reinforcement layer; x = horizontal distance along the reference axis of each element; a_i, b_i and c_i = coefficients for determining the shape of the quadratic curve; and $i = 1 \sim m$.

4.3 Displacement functions and their derivatives

The prestressed concrete beam elements used in this study are shown in Fig. 3. The displacement functions of the incremental displacements Δu, Δw and ΔS_i ($i = 1 \sim m$) are

$$\left.\begin{array}{rcl} \Delta u &=& [\,1 \quad x\,]\{\,\alpha_{u1} \quad \alpha_{u2}\}^T = [\,f_u\,]\{\,\alpha_u\,\} \\ \Delta w &=& [\,1 \quad x \quad x^2 \quad x^3\,]\{\alpha_{w1} \quad \alpha_{w2} \quad \alpha_{w3} \quad \alpha_{w4}\,\}^T = [\,f_w\,]\{\,\alpha_w\,\} \\ \Delta S_i &=& [\,1 \quad x\,]\{\,\alpha_{s1} \quad \alpha_{s2}\}^T = [\,f_{si}\,]\{\,\alpha_{si}\,\} \end{array}\right\} \tag{5}$$

where $\{\alpha_u\}$, $\{\alpha_w\}$ and $\{\alpha_{si}\}$ are the generalized displacements of Δu, Δw and ΔS_i, respectively; and $i = 1 \sim m$.

Thus, the derivative functions of these incremental displacements that are needed in the subsequent formularization are

$$\left.\begin{array}{l} \frac{d\Delta u}{dx} = [\,f_u'\,][\,C_u^{-1}\,]\{\,\delta u\,\} \\ \frac{d\Delta w}{dx} = [\,f_w'\,][\,C_w^{-1}\,]\{\,\delta w\,\} \\ \frac{d^2\Delta w}{dx^2} = [\,f_w''\,][\,C_w^{-1}\,]\{\,\delta w\,\} \\ \frac{dS_i}{dx} = [\,f_{si}'\,][\,C_{si}^{-1}\,]\{\,\delta S_i\,\} \end{array}\right\} \tag{6}$$

where $\{\delta u\}$, $\{\delta w\}$ and $\{\delta S_i\}$ = the incremental nodal displacement vectors for Δu, Δw and ΔS_i, respectively; $[\,C_u^{-1}]$, $[\,C_w^{-1}]$ and $[\,C_{si}^{-1}]$ = the inverse matrices of the well-known matrix $[\,C]$ for Δu, Δw and ΔS_i, respectively; and $i = 1 \sim m$.

4.4 Incrementalized finite element equation

By substituting the relationship between Eqs. (4)$\sim$(6) into the Eq. (3), we get the following incrementalized finite element equation for material nonlinear analysis of prestressed concrete beams:

$$\begin{bmatrix} K_{uu} & K_{uw} & K_{uS} \\ K_{uw}^T & K_{ww} & K_{wS} \\ K_{uS}^T & K_{wS}^T & K_{SS} \end{bmatrix} \begin{Bmatrix} \delta u \\ \delta w \\ \delta S \end{Bmatrix} = \begin{Bmatrix} \delta P_u \\ \delta P_w \\ \delta P_S \end{Bmatrix} \tag{7}$$

where $\{\delta S\}$ = the incremental slip displacement vector of the nodes with respect to all reinforcement m layers; and $\{\delta P_u\}, \{\,\delta P_w\}$ and $\{\delta P_S\,\}$ = the incremental load vectors corresponding to the displacement vector $\{\delta u\}$, $\{\delta w\}$ and $\{\delta S\}$, respectively.

4.5 Nonlinear solution procedure

An increase in the deformation of prestressed concrete beams due to an increase in load leads to the occurrence of various nonequilibrium stresses inside the members due to such factors as cracking in the concrete, yielding

of the reinforcements, and progression of bond-slip between the reinforcements and concrete. These, in turn, lead to further deformation. In this study, an analytical program using the incremental displacement method as well as the incremental load method was developed for nonlinear analysis.

5 Numerical examples

(1) Example 1

First, in order to test the fitness of our analytical method, beam A was selected from Lin's series(1955) of post-tensioned bonded continuous beams for the static load test. The outline of this beam is shown in Fig. 4(a). As is clear from the figure, this beam is a two-span continuous beam. The tendon profile used in the calculations and the material properties of the concrete, tendons, etc. are also shown in this figure. In order to conduct nonlinear analysis under conditions of external loading on the beam, we first conducted jacking analysis of the tendons (P_{so}= 130 *kips*), and then loading analysis after hardening of the grouted cement paste was performed. For the calculations, the beam was divided into 86 elements of almost equal length in the member axis direction, and each element was subdivided into

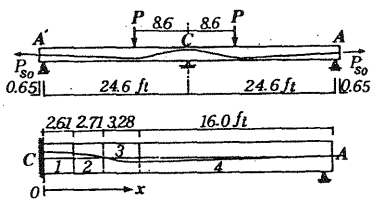

CONCRETE:
E_{co} = 5400 *ksi*(*jacking*), E_{co} = 5550 *ksi*,
f_c = 6400 *psi*, f_{ct} = 510 *psi*, ϵ_{cc} = 0.003
TENDON:
A_{si} = 0.963 in^2, E_s = 27000 *ksi*,
H_s = 0.0025E_s, σ_{sy} = 227 *ksi*
BOND-SLIP:
by CEB-FIP model code.

(a) Beam Outline and Material Properties

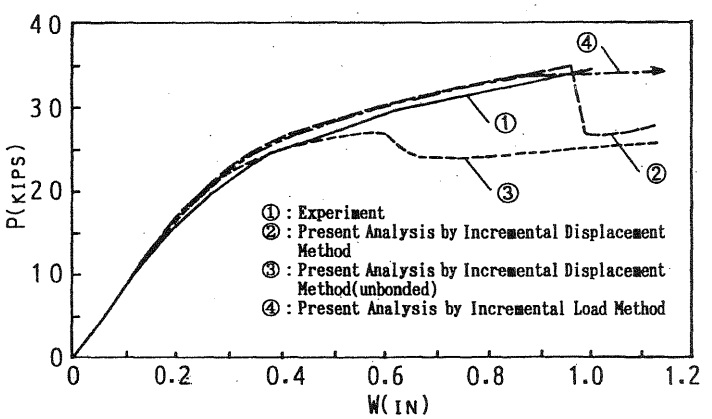

(b) Midspan Load-Displacement Curve

Fig. 4. Analysis of Lin's Beam(1 *in.*=2.54 *cm*; 1 *Kip*=4.45 *KN*)

20 layers in the thickness direction of the beam. The midpoint load-displacement curve due to the increasing concentrated load P is shown in Fig. 4(b). The analytical values calculated by the incremental displacement method in the case of a bonded or unbonded state between the tendons and concrete(grouted cement) are plotted. For comparison, the values calculated by the incremental load method in the case of a bonded state between the tendons and concrete are also plotted.

The following interesting conclusions can be drawn from a comparison of the curves in Fig. 4(b): 1) The values calculated by the incremental displacement method and the incremental load method both show the general load-displacement behavior of the beams with relatively high accuracy. However, the deformation calculated by the incremental load method flows near the peak load, and the amount of beam deformation at peak load is not clear. The values calculated by the incremental displacement method, in contrast, clearly show not only the amount of displacement at peak load but also the deformation behavior in the post-peak load range. Whether or not these values approximate the true phenomena, however, is not clear because experimental values are not shown. 2) If we compare the values calculated by the incremental displacement method in the case of a bonded or unbonded state between the tendons and concrete, we can observe the effects that the bonding action between tendons and concrete have on the load-displacement behavior of the beam. Of particular interest is that these two values dramatically reduced load bearing capacity after showing peak load, and in the subsequent range of stabilization and gradual increase of the analytical curve, both values remained almost constant, suggesting that at this point bond fracturing has almost finished.

(2) Example 2

Umezu et al.(1995) tested a two-span continuous prestressed concrete beam with external tendons under static load up to failure. They also presented an analytical procedure to predict the behavior of these beams. In order to show a numerical example of a prestressed concrete beam with external tendons, we analyzed such a beam. Fig. 5(a) shows an outline of the beam and physical properties of the materials used in the beam. Fig. 5(b) and (c) show midspan load-displacement and the increasing force curve of the external tendons at the anchoring point, respectively, accompanying an increase in load. Each of these figures shows our analytical values (calculated by the incremental displacement method) and experimental values, as well as the analytical values of Umezu et al.(1995) A comparison of the midspan load-displacement curves in Fig. 5(b) clearly shows that the analytical value of the amount of displacement at peak load calculated by the incremental displacement method is slightly smaller than the experimental

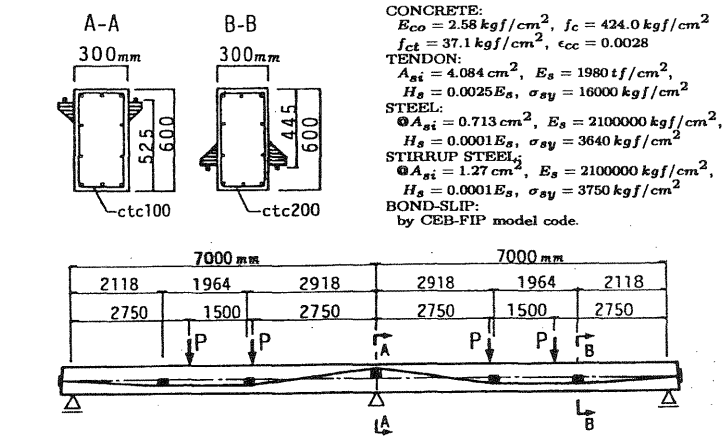

(a) Beam Outline and Material Properties

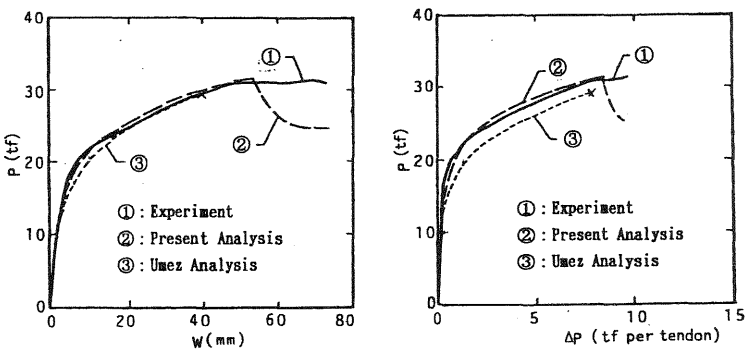

(b) Midspan Load-Displacement Curve (c) Load-Increasing Tendon Force

$(1\,kgf/cm^2 = 0.098\,Mpa; 1\,kgf = 9.8N; 1\,tf = 9.8\,KN)$

Fig. 5. Umezu Beam Analysis

value. However, despite this small difference, it is clear from these figures that our analytical method can accurately show the general behavior of a prestressed concrete beam with external tendons.

6 Summary and conclusions

We proposed a material nonlinear analytical method, based on the finite element method, for prestressed concrete beams with curved tendons (also applicable to framed structures) that takes into account the bond-slip action of reinforcements. This method can be used to predict the displacements, stresses and strains acting on the concrete and reinforcements, and the bond stresses and slips between the concrete and reinforcements in such beams through all ranges of elastic, inelastic, peak load and post-peak load.

The accuracy of the proposed analytical method was verified by numer-

ical examples.

Since all possible bond-slip actions of prestressing tendons are considered in our analytical method, it is possible to trace the variation in prestress during various stages of jacking and loading in a unified manner.

7 References

CEB(1993)-FIP Model code 1990.

Kang,Y.J. and Scordelis,A.W.(1980) Nonlinear analysis of prestressed concrete frames. **ASCE**, 106, ST2, 445-462.

Lin,T.Y.(1955) Strength of continuous prestressed concrete beams under static and repeated loads. **ACI Journal**, 26(10), 1037-1059

Nishiyama, M., Muguruma, H. and Watanabe, F. (1988) Hysteretic restoring force characteristics of unbonded prestressed concrete framed structure under earthquake load. in **Pacific Concrete Conference** (eds. R. Park et al.), New Zealand, 101-112.

Okamura, H. and Maekawa, H.(1991) **Nonlinear analysis and constitutive models**, Gihodo, Tokyo.

Park, R., Priestley M.J.N. and Gill W.D. (1970) Ductility of square-confined concrete columns. **ASCE**, 108, ST4, 929-950.

Saenz,L.P.(1974) Discussion of "Equation for the stress-strain curve of concrete, by Desay,P. and Krishna,S.", **ACI Journal**, 61(9), 1229-1235.

Tanabe, T. and Hong, P.W.(1980) Unbonded precastelements and its skeletal assemblage. **Proc. of JSCE**, 303, 133-142.

Uchida, Y., Rokugo, K. and Koyanagi, W.(1991a)Determination of tension softening diagrams of concrete by means of bending tests, **Proc. of JSCE**, 426/14, 203-212.

Ueda, M. and Dobashi, Y.(1985) Nonlinear bond slip analysis of axially loaded reinforced concrete prismatic members. **Proc. of JSCE**, 360/3, 71-80.

Ueda, M.(1990)Governing equations of prestressed concrete beams with curved tendons and its numerical examples by the finite element method. **Conc. Res. and Tech.**, 1-1, 11-24.

Umezu, K. et al. (1995) A study on the ultimate flexual strength of 2-span continuous beam using external cables. **Proc. of JCI**, 17(2), 743-748.